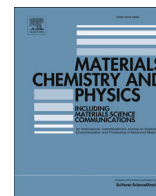




Contents lists available at ScienceDirect

## Materials Chemistry and Physics

journal homepage: [www.elsevier.com/locate/matchemphys](http://www.elsevier.com/locate/matchemphys)

## Tribological and mechanical investigation of acrylic-based nanocomposite coatings reinforced with PMMA-grafted-MWCNT

A. Al-Kawaz<sup>a</sup>, A. Rubin<sup>a,\*</sup>, N. Badi<sup>a</sup>, C. Blanck<sup>a</sup>, L. Jacomine<sup>a</sup>, I. Janowska<sup>b</sup>,  
C. Pham-Huu<sup>b</sup>, C. Gauthier<sup>a</sup>

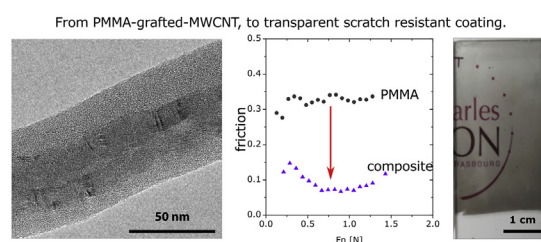
<sup>a</sup> UPR22/CNRS, Institut Charles Sadron, Université de Strasbourg, 23 Rue du Læss, BP 84047, F-67034 Strasbourg Cedex 2, France

<sup>b</sup> Institute of Chemistry and Processes for Energy, Environment and Health (UMR 7515) CNRS - University of Strasbourg, 25 Rue Becquerel Strasbourg, 67087 Cedex 08, France

### HIGHLIGHTS

- Synthesis of MWCNT-PMMA nanoparticles by ATRP “grafting from” approach.
- PMMA-grafted-MWCNT/PMMA coatings with good mechanical properties.
- High tribological performance of PMMA-grafted-MWCNT/PMMA coatings.

### GRAPHICAL ABSTRACT



### ARTICLE INFO

#### Article history:

Received 10 December 2015

Received in revised form

10 March 2016

Accepted 19 March 2016

Available online xxx

#### Keywords:

Polymers  
Composite materials  
Nanostructures  
Surface properties  
Tribology  
Friction

### ABSTRACT

The chemical functionalization of carbon nanotubes (CNTs) could improve their chemical compatibility. Poly(methyl methacrylate) (PMMA)-functionalized multi-walled carbon nanotubes (MWCNTs) are prepared by in situ atom transfer radical polymerization (ATRP) using a “grafting from” approach. It allows the control of the thickness of the polymer layer grafted on MWCNTs from two parameters: the feed ratio of MMA to MWCNT, the volume fraction of solvent to MMA. This work compared the effect of several PMMA-grafted-MWCNT fillers embedded into a PMMA matrix, PMMA-grafted-MWCNT/PMMA, and obtained by solution mixing technique. We studied the tribological performances of 20  $\mu\text{m}$  coatings of these nanocomposites deposited on neat PMMA. The percentage of embedded fillers is kept low to maintain the transparency of the PMMA. The coefficient of friction was found to relatively decrease with the increase of the weight fraction of polymer grafted to the surface of MWCNT. Moreover the elastic modulus also increased with increasing the weight fraction of PMMA coated MWCNT.

© 2016 Elsevier B.V. All rights reserved.

### 1. Introduction

Most polymeric materials exhibit low resistance to scratching and marring, and thus are not suitable for many industrial applications. Therefore, there is a constant need in improving surface

properties (i.e. resistance to scratch etc.) and coating is an interesting solution [1–3]. Indeed there is no polymer in a pristine form that can provide a reasonable low working wear rate with an optimum coefficient of friction. That is why polymeric coatings used in tribological applications are modified by suitable fillers to reduce the friction coefficient (wear rate), to improve their strength and their elastic modulus. These fillers are designed to introduce an elastic contribution into a fully plastic behavior or to increase the elastic component in an elastic–plastic behavior of the coating [4].

\* Corresponding author.

E-mail address: [anne.rubin@ics-cnrs.unistra.fr](mailto:anne.rubin@ics-cnrs.unistra.fr) (A. Rubin).

Poly(methyl methacrylate) (PMMA) is a widely used polymer in architecture, automotive or railways glazing, as well as biomedical sector due to its good optical, mechanical and biocompatibility properties. Nonetheless it has a low wear resistance. The main issue is therefore to optimize a PMMA-based composite coating that protects the surface with minimum loss in optical transparency.

Carbon nanotubes (CNTs) which were discovered by Iijima in 1991 [5,6] have excellent mechanical properties which could be efficiently used as nano-fillers. The high aspect ratio of nano-fillers leads to very large effective surface area and favors their use as reinforced particles in a polymer matrix (nano-composite). Polymer nano-composites do not always have mechanical properties enhancement compared to the neat polymer but a low reinforced CNTs content can be sufficient provided that fillers' dispersion is homogeneous and interaction between the matrix and the nanoparticles is high enough [7,8]. In such case, the use of a low percentage of CNTs in the nanocomposite's coating dedicated to tribological applications is interesting to keep the transparency at best [3]. The tricky point is therefore to choose the best chemical route to modify the CNTs surfaces to prevent both CNTs aggregation and weak bonds with the host matrix. Two classical approaches are possible: covalent or non-covalent surface modifications. Non-covalent bonding can be performed by the use of surfactants or block copolymers [9–11], or by solvent free ionic liquid dispersion [12,13]. Covalent bonding can be created on multi-walled carbon nanotubes (MWCNTs) with functional groups like COOH, amine, silane, etc. [14]. Attachment of small molecules or doping has resulted in significant development of CNTs application in several fields including composites, energy storage and catalysis [15–19]. Moreover, their compatibility with polymer matrices was considerably enhanced by the direct introduction of macromolecules onto the surface of CNTs [20]. For the case of PMMA, several routes are reported. Kong et al. presented a novel in situ atom transfer radical polymerization (ATRP) ("grafting from" approach) to functionalize MWCNTs with PMMA chains [21]. The PMMA-grafted-MWCNT showed a relatively good solubility in none or weakly polar solvents such as tetrahydrofuran (THF) and chloroform (CHCl<sub>3</sub>) and a poor solubility in strong polar solvents such as dimethylformamide (DMF) and dimethyl sulfoxide (DMSO). Interestingly, Hwang et al. reported that the incorporation of PMMA-grafted-MWCNTs to commercial PMMA, realized by dissolution techniques, leads to a better dispersion of the filler in the matrix and an increase in bulk mechanical properties [22]. They measured a significant increase of the storage modulus (1100%) for PMMA reinforced with 20 wt.% PMMA-grafted-MWCNT at 20 °C. The matrix/nanoparticles interaction was therefore strong and ensured a load transfer from the polymer matrix to the MWCNTs. These bulk tendencies were confirmed by Wang et al. who performed the incorporation of low percentage of PMMA-grafted-MWCNTs [0.5–2 wt.%] to poly(styrene-co-acrylonitrile), realized by solution casting from THF [23]. For example, at 40 °C this improvement was of a factor 2 for the elastic modulus and a factor 6 for the toughness. Their observations also led to the conclusion that best mechanical improvement is reached for an optimum MWCNTs content. For lower PMMA-grafted-MWCNTs amount (i.e. lower than 0.5 wt.%) Blond et al. showed that the Young's modulus, tensile strength and toughness were improved by 1.9, 4.6, and 13.7 times, respectively [24]. Even at low percentage of fillers grafted with macromolecules, it is possible to enhance the bulk mechanical properties of a nano-composite. The question which still awaits for an answer is does such nano-composite still ensures good tribological properties?

A huge amount of studies on the tribological behavior of polymer nano-composites exist, nonetheless fewer deals with tribological performances of acrylic-based nano-composites coatings. Dong et al. measured a significant decrease of the friction

coefficient (~30% for 2.5 weight percent with respect to the monomer) and the wear rate for 1% of CNTs incorporated in a PMMA matrix by an in situ polymerization process [25]. More recently Kim et al. performed tribological experiments on polyimide-based coatings reinforced with 1, 3 and 5 wt.% PMMA-grafted-MWCNT [26]. These coatings were confined between a steel ball and an aluminum substrate at 0.9 GPa contact pressure and sheared at 0.02 m/s sliding speed. Only the one containing 3wt.% PMMA-grafted-MWCNT gave valuable results (some delamination occurred on the other ones). As the coating thickness is not known, it does not give information on the elastic component brought by the reinforcement fillers.

The question is, how could we control at best the growth of the PMMA-grafted macromolecules on carbon nanofillers to see an effect of the coating elastic component during shearing? Mameri et al. introduced methyl methacrylate as a functional group on MWCNT surfaces and showed that controlling its length led to a better miscibility of CNTs in common organic solvents and in polar polymers like PMMA. They showed that the use of longer macromolecules led to a decrease of the free volume and hence the chain mobility, inducing higher elastic modulus and hardness in nano-composite [27]. In this work, we study the effect of increasing the thickness of grafted polymer layer on the MWCNTs surface upon properties of PMMA composites. MWCNT-grafted PMMA/PMMA nano-composites were prepared by a solution mixing process. Mechanical and tribological characterizations of the composites were achieved by the use of nanoindentation tests and a custom-made scratching test that allows in situ observation of the contact during scratching.

## 2. Materials and methods

### 2.1. Materials

The initiator 2,2'-azobisisobutyronitrile (AIBN), 2-bromo-2-methylpropionyl bromide, thionylchloride (SOCl<sub>2</sub>), N,N,N',N',N''-pentamethyldiethylenetriamine (PMDETA), N,N-dimethylaminopyridine (DMAP) and methanol were purchased from Sigma–Aldrich and used as received. Functionalized carbon nanotubes (MWCNT-COOH and MWCNT-OH) were purchased from Nanocyl SA and used without further purification. The monomer methyl methacrylate (MMA – 99%) was purchased from Sigma–Aldrich and distilled in order to remove the stabilizer prior to use. CuBr was purchased from Sigma–Aldrich and cleaned with glacial acetic acid, filtered and washed with ethanol in order to remove any oxidized species. Tetrahydrofuran (THF), N,N-dimethylformamide (DMF), glycol (HOCH<sub>2</sub>CH<sub>2</sub>OH) and chloroform (CHCl<sub>3</sub>) purchased from Sigma–Aldrich were distilled before their use.

### 2.2. Preparation of functionalized MWCNTs with PMMA by "grafting-from" method

*In situ* atom transfer radical polymerization (ATRP) "grafting from" approach was used to functionalize MWCNTs with PMMA chains [12]. The general strategy for grafting polymers from the MWCNTs via in situ ATRP can be realized by five steps as sum-up in Fig. 1.

**(i) Preparation of MWCNT-COOH:** The pristine MWCNTs (with 30–50 nm outer diameter and 10–20 μm length) contain 0.75% of COOH group. The first step consisted in eliminating impurities from the MWCNTs (such as metallic catalysts) and producing MWCNTs-COOH with high percentage of carboxylic groups. 1 g pristine MWCNTs were treated with 10 mL of 68%-HNO<sub>3</sub>

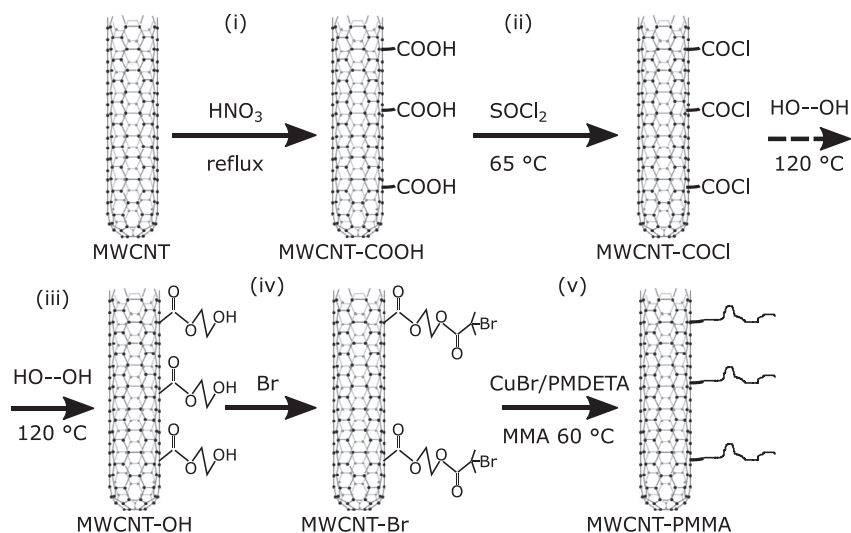


**Fig. 1.** Strategy for the modification of carbon nanotubes using atom transfer radical polymerization (ATRP): (i) 68% HNO<sub>3</sub> aq., 100 °C, 24 h; (ii) SOCl<sub>2</sub>, 65 °C, 24 h; (iii) glycol, 120 °C, 48 h (iv) 2-bromo-2-methylpropionyl bromide, chloroform, 48 h; (v) CuBr, PMDETA, MMA, DMF, 60 °C, 24 h.

aqueous solution for 30 min in a sonication bath. Then the solution was refluxed for 24 h at 100 °C. The resulting dispersion was diluted in water and filtered. The resulting solid was washed up to neutral pH and dried under vacuum at 40 °C overnight. These acid-treatments are known to shorten the length of MWCNTs and introduce hydroxyl functional groups to MWCNTs. It also makes MWCNTs more dispersible in common organic solvents.

**(ii) Generation of MWCNT-COCl from MWCNT-COOH:** Functionalized MWCNTs with carbonyl chloride groups (MWCNT-COCl) were prepared via reaction of thionylchloride (SOCl<sub>2</sub>) with carboxyl-contained MWCNTs (MWCNT-COOH). Typically 0.6 g of MWCNT-COOH were suspended in 20 mL of SOCl<sub>2</sub> under stirring at 65 °C for 24 h under N<sub>2</sub>. The residual solid was then separated by filtration and washed with anhydrous THF. The solid was dried under vacuum at room temperature for 2 h.

**(iii) Synthesis of MWCNT-OH from MWCNT-COCl:** For the third step, hydroxyl groups were introduced onto the surface of MWCNTs by the reaction of MWCNT-COCl with glycol generating MWCNT-OH. Typically 0.5 g of MWCNT-COCl was mixed with 20 mL of glycol and stirred at 120 °C for 48 h. The solid was separated by vacuum filtration with 0.22 μm Millipore polycarbonate membrane. The resultant solid was washed with anhydrous THF three times and then dried under vacuum at room temperature overnight.

**(iv) Synthesis of MWCNT-Br from MWCNT-OH:** In a fourth step, reactive sites (MWCNT-Br) for ATRP were formed by mixing 0.5 g MWCNT-OH, 10 mL of distilled CHCl<sub>3</sub>, 0.0365 g of DMAP and 0.303 g of triethylamine. Then 0.684 g of 2-bromo-2-methylpropionyl bromide dissolved in 5 mL CHCl<sub>3</sub> was added drop wise at 0 °C in 60 min. The mixture was stirred for 3 h at 0 °C followed by stirring at room temperature for 48 h. Then the solid was separated from the mixture by filtration, washed with CHCl<sub>3</sub> five times and dried under vacuum at 40 °C overnight.

**(v) Synthesis of MWCNT-PMMA from MWCNT-Br:** The final step was the synthesis of PMMA-grafted-MWCNT. Typically, 0.1 g MWCNT-Br and 0.0286 g of CuBr were placed in a 10 mL dried flask. In another dried flask 0.03466 g of PMDETA and 1.014 g MMA were mixed to 1 mL of DMF. Both flasks were sealed with a rubber stopper. The flasks were degassed and backfilled with argon three times. Then the mixture of MMA and PMDETA in DMF was injected into the first flask using a

degassed syringe. The flask was immediately immersed in an oil bath at 60 °C and stayed under continuous stirring for 24 h. The mixture was diluted with CHCl<sub>3</sub> and filtered under vacuum with a 0.22 μm Millipore polycarbonate membrane filter for three times.

The thickness of the polymer layer grafted on the MWCNTs can be controlled by the feed ratio of MMA to MWCNT-Br. Table 1 summarizes the tested conditions for the PMMA functionalization.

### 2.3. Preparation of acrylic MWCNTs composites coatings

Acrylic-based composites were prepared with poly(methyl methacrylate) using a solution mixing technique. Solution process begun with the dispersion of MWCNT-PMMA fillers in a solvent, typically THF, by tip sonication (40% power) for 20 min followed by bath sonication at room temperature for 3 h. This solution is mixed with PMMA powder dissolved in the same solvent (1 g/10 mL) and dispersed by shear mixing (Silverson shear mixer, Silverson machines) at 6500 rpm for 60 min in an ice bath to reduce the frictional heat produced in the polymer by the shear mixer. The composite solution of PMMA was then coagulated with cold methanol (300 mL), filtered under vacuum and dried overnight to yield a solid flaky material.

Two coated samples were prepared. A first set was deposited on microscope glass blades to characterize the bulk mechanical properties of the coating by nanoindentation tests. A second set was deposited on commercial PMMA samples (Arkema) to perform friction experiments. The coating's solution was obtained from the resultant composite powder dissolved in dry THF with the ratio (1 g/5 mL) and well dispersed in a shear mixer for minimum 10–15 min. Prior to deposition the glass slides were cleaned by immersion in Piranha solution (mixture of H<sub>2</sub>SO<sub>4</sub>:H<sub>2</sub>O<sub>2</sub>, 3:1) for 24 h and another 24 h in the solution (HCl 1 mL: water 2 mL). Finally the glass was washed with distilled water and kept in an oven for drying. The PMMA substrates were cleaned with ethanol and dried under N<sub>2</sub> before the coating process. All coatings were deposited by the Doctor Blade technique to obtain top coats of 15–20 μm (Fig. 2). All coated samples were dried at ambient temperature for 24 h and then at 70 °C under vacuum for 48 h.

**Table 1**  
Experimental conditions used in order to functionalize MWCNT with PMMA chains.

Sample	Feed ratio <sup>a</sup>	Monomer catalyst ligand <sup>b</sup>	Monomer solvent <sup>c</sup>	Temp. (°C)	Reaction time (h)	TGA weight fraction loss (%) <sup>d</sup>
#1 <sup>e</sup>	10:1	50:1:1	1:10	60	24	/
#2 <sup>f</sup>	10:1	50:1:1	1:5	60	24	49.1
#3 <sup>f</sup>	10:1	50:1:1	1:1	60	24	65.5
#4 <sup>f</sup>	20:1	100:1:1	1:1	60	24	71.5

<sup>a</sup> Monomer:MWCNT-Br (wt.:wt.).

<sup>b</sup> monomer:CuBr:PMDETA (mol:mol:mol).

<sup>c</sup> monomer:solvent (v:v).

<sup>d</sup> L% the loss weight fraction of polymer calculated from TGA data.

<sup>e</sup> Functionalization starting from commercially available MWCNT-OH.

<sup>f</sup> Rom commercially available MWCNT-COOH.



**Fig. 2.** 2 wt.% PMMA-grafted-MWCNT/PMMA coating of 15–20  $\mu\text{m}$  on glass substrate obtained by Doctor Blade technique (samples with different monomer:MWCNT-Br ratio (wt.:wt.); monomer:CuBr:PMDETA ratio (mol:mol:mol) and monomer:solvent ratio (v:v) see Table 1 type #2, #3, #4).

#### 2.4. Characterization techniques

Structure chemistry of our pristine and modified fillers was measured by Fourier Transform Infrared Spectroscopy (FTIR), Photoelectron Spectroscopy (XPS) and Thermogravimetric Analyses (TGA). The FTIR apparatus was a Nicolet 6700 spectrometer (Thermo Fisher Scientific, USA). The samples were prepared with KBr disks and the scanning range was from 400 to 4000  $\text{cm}^{-1}$ . The XPS measurements were performed on an ESCA-2000 System (VG Microtech). The data were obtained using a monochromatized aluminum K $\alpha$  anode. The TGA analyses were realized on a METTLER TC10 A TG50. The analyzer was heated up to 800 °C under 1 atm of air pressure with a heating rate of 20 °C/min.

The PMMA grafting on MWCNTs was also checked by Transmission Electron Microscopy (TEM). Functionalized and unfunctionalized MWCNTs were dispersed in THF solvent and the solution was sonicated during 10 min. Five microliters of the solution were deposited onto a Lacey-Formvar/carbon-covered copper grid (300 mesh). The suspension was left for 2 min and finally dried using a filter paper. TEM imaging was carried out using a Technai G2 microscope (FEI) at 200 kV. Images were acquired with an Eagle2K slow-scan charge-coupled device (ssCCD) camera (FEI).

Coatings mechanical properties were measured by a depth-sensing nanoindentation technique. The measurements were performed using an Ultra Nano Hardness Tester (UNHT, Anton-Paar TriTec, Switzerland) with a normal load range of 0.1 mN–500 mN (resolution 0.04  $\mu\text{N}$ ) and a maximum depth of 200  $\mu\text{m}$  (resolution 0.04 nm). Measurements were carried out at room temperature with a Berkovich tip (diamond three-sided pyramid). It should be noted that to get the intrinsic mechanical properties of the coating the indentation depth must be lower than one tenth of the coating thickness that is approximately 1.5  $\mu\text{m}$  for our samples. For each

sample a matrix with 8 identical indentations was programmed to get good statistics. Each indentation corresponded to some loading–unloading cycles. To avoid viscoelastic effect, it consisted of ten successive cycles of progressive loading: the first cycle started at 0.5 mN loading for 50 s, it was then unload to 5% of the value and remained unloaded for 50 s. This normal load reduction allowed partial or complete relaxation before starting a second cycle. These steps were repeated 10 times until the final load reached 30 mN. Tribological experiments were carried out on a home-made sclerometer, the Micro-Visio-Scratch apparatus (MVS). This set-up is completely described elsewhere [28,29]. The input parameters are normal load  $F_n$  (0.05 N–25 N), tip geometry, temperature and sliding speed ( $10^{-3}$  mm/s to 15 mm/s). The contact area is photographed in situ at every loading step. Fig. 3 displays a classical contact shape which can be symmetrical (elastic range) or asymmetrical (elastic–plastic or fully plastic range). The contact strain  $\epsilon$  is directly calculated from this photograph as it is proportional to the ratio  $a/R$  where  $a$  is the radius of the contact and  $R$  the radius of the indenter ( $\epsilon = 4/3\pi \cdot a/R$  for an elastic contact and  $0.2 a/R$  for the other). Measurements were performed at low relative humidity ( $\text{RH} < 4\%$ ), ambient temperature and constant sliding speed (0.03 mm/s) with a diamond indenter whose radius is 98  $\mu\text{m}$ .

### 3. Results and discussion

#### 3.1. PMMA functionalization of commercial MWCNT-OH

In a first study, commercially available MWCNT-OH containing around 4.7% OH groups was modified with PMMA, following the protocol described in the experimental section (steps (iv) and (v)). The surface chemical compositions of both the unmodified and

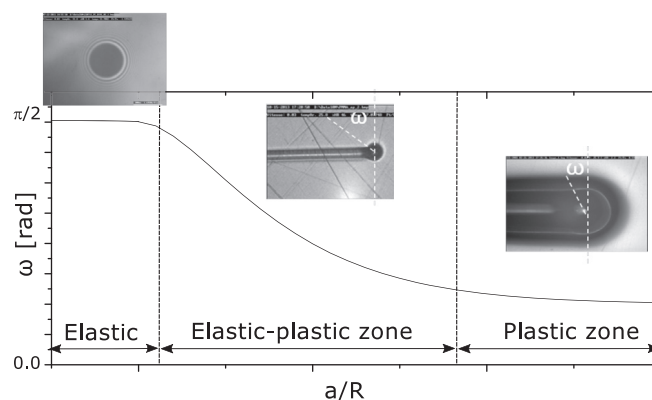


**Fig. 3.** Sketch of typical snapshots during sliding of a spherical rigid indenter on a transparent polymeric surface in the elastic, elasto-plastic and plastic regime. The omega angle  $\omega$  is characteristic of the rate of plastic flow in the contact.



**Table 2**

Elemental atomic composition of the different chemical species present on the modified MWCNT after acid treatment, and after bromide reaction, measured by XPS.

Route	Product	Synthesis way	O%	C%	Br%
1 (iv–v)	MWCNT-OH	Commercial	4.7	95.3	0
	MWCNT-Br	Lab.	5.2	94.76	0.04
2 (i–v)	MWCNT-PMMA	Lab.	4.31	95.69	/
	MWCNT-COOH	Commercial	4.0	/	/
	MWCNT-COOH	Lab.	10.99	89.01	0
	MWCNT-Br	Lab. (type#2)	10.23	87.88	1.89
	MWCNT-PMMA	Lab. (type#2)	17.97	82.03	/

modified MWCNTs were determined by XPS analysis (Table 2). It can be seen from the data in Table 2 that the Br content was only 0.04% in the resulting MWCNT-Br. The reason for the low

percentage of Br can be attributed to the low percentage of hydroxyl groups in the commercial MWCNT-OH (only 4.7%) and their non-easy accessibility in non-homogeneous systems. Therefore, the functionalization with PMMA was also unsuccessful as confirmed by TEM results (Fig. 4A). Indeed, PMMA functionalization was achieved using the MWCNT-Br as initiator of the atom transfer radical polymerization of methyl methacrylate (grafting from approach). In general, decreasing the amount of initiator (i.e. Br groups in this case) leads to the increase of PMMA molecular weight. However, in this study, it seems more likely that the weak amount of Br sites lead to a non-success of the polymerization process even if no Br groups remained. Indeed, no clear change of the nanotubes surface was observed after PMMA functionalization, thus proving a non-success of the PMMA functionalization (Fig. 4A–b). Increasing the reaction time from 24 h to 48 h or 72 h did not have a significant effect on these results.

The nature and concentration of the oxygenated functional groups decorating the surface of the MWCNT after acid treatment determined by XPS are presented in Fig. 5. The survey and high resolution O1s XPS spectra (Fig. 5) clearly evidence the presence of several C–O species on the acid treated sample in good agreement with the results reported in the literature. It is expected that these oxygenated functional groups, and especially COOH groups, will participate in a large extend to the anchorage of the PMMA on the tube surface.

Therefore, a second strategy consisting in 5 steps (steps (i) to (v) in the experimental section) was tested in order to increase the hydroxyl content of the MWCNT leading to a higher anchorage sites for PMMA. This second process started with a commercially available MWCNT-COOH containing about 4% carboxyl groups (Table 2). After an acidic treatment, an increase of the carboxyl group's content from 4% to 11% was observed according to the XPS analysis (Fig. 5). Table 2 presents the results for the sample #2 as an example, it is alike for #3 and #4. The use of this new MWCNT-COOH resulted in the formation of MWCNT-Br with higher Br content (1.89% instead of 0.04%). This result may be attributed to an increase of the density of hydroxyl groups on the MWCNT surface following the increase of the carboxyl group's content. ATRP was then conducted on this new MWCNT-Br. The XPS measurements after polymerization showed the complete disappearance of the Br groups. The high PMMA decoration of the acid treated MWCNT also confirms the results obtained above and is shown by the TEM analysis presented in the Fig. 4. TEM micrographs in panel B, Fig. a) to d), show the microstructure of the MWCNT obtained via route 2. PMMA-grafted MWCNT (samples #3 & 4 from Table 1) were compared to non-functionalized MWCNT (MWCNT-COOH and MWCNT-Br) in order to detect a possible increase of MWCNT surface thickness. The TEM micrograph of the acid treated MWCNT in Fig. 4B–a evidences a similar tube morphology after acid treatment (black arrow) and confirms the treatment is non destructive. The same microstructure was again observed by TEM (black arrow) on the same tube after Br adding (Fig. 4B–b) indicated that no damage was resulted during the bromide addition step (see also SI). TEM micrographs in Fig. 4B–c and 4 B–d show the microstructure of the grafted MWCNT after the step v).

TEM analysis clearly shows the formation of a low ordered material on the outer surface of the tube: the presence of a PMMA layer on the tube wall embedded the MWCNT with a variable thickness (10–30 nm in thickness - see also SI for micrographs at higher magnification). The white arrow points to the PMMA and the black one's to the carbon layers underneath. However, the thickness of the polymer layers was not homogeneous along the tube wall as well as between tubes, therefore it was not possible to calculate precisely their average thickness. Such phenomenon could be attributed to an inhomogeneous mixing of the MWCNT

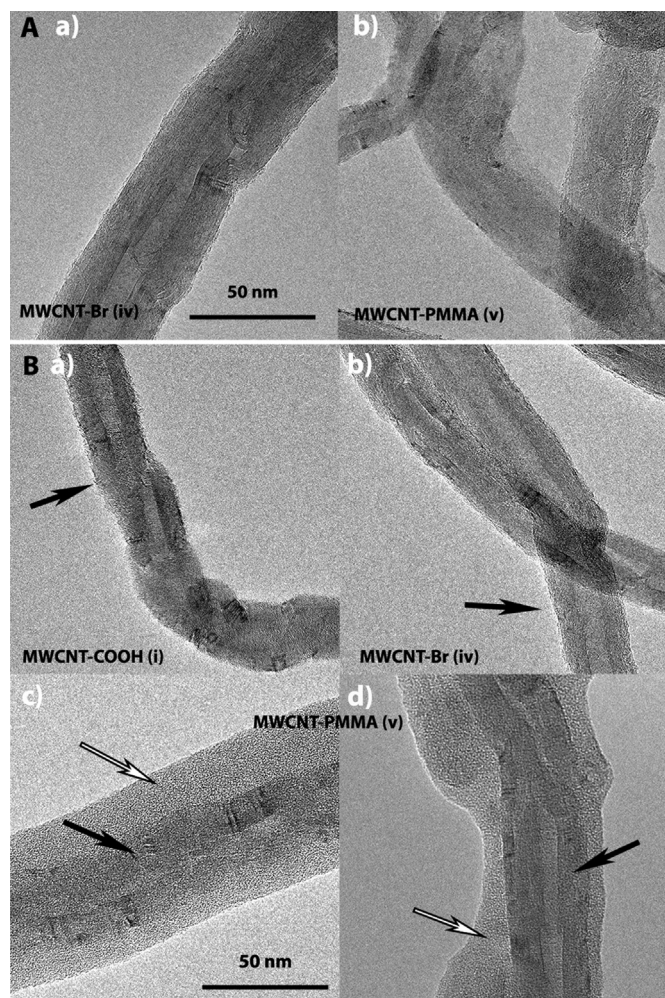


**Fig. 4.** TEM images of the different steps of the grafting procedure of PMMA onto the MWCNT. In panel A route 1 is represented. a) present a characteristic MWCNT-Br from the step iv). The walls of the MWCNT are clearly seen and no modification is observed at the outer surface. b) represent step v) which is the grafting of PMMA. On the different images observed no material is seen attached to the outer surface of the MWCNT. Panel B represents MWCNT obtained via route 2. a) MWCNT-COOH on which the carbon layer are seen - black arrow (see also SI). b) After step iv) no differences are seen by TEM and the walls of the tube seem intact (black arrow). Image c) and d) show the MWCNT after the step v), in that case the grafted PMMA is clearly seen as an amorphous layer embedding the MWCNT with a variable thickness (10–30 nm in thickness). The white arrow points to the PMMA and the black one's to the carbon layers.

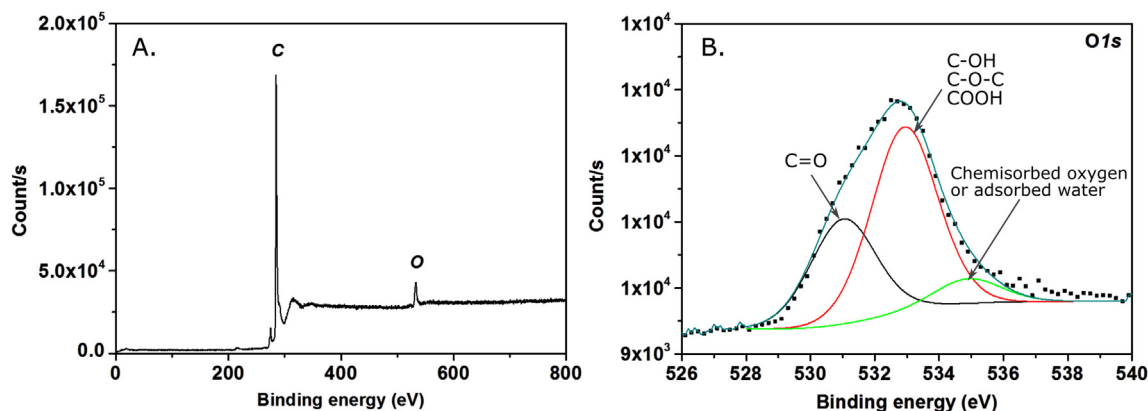


Fig. 5. (A) XPS survey spectrum and (B) high resolution XPS spectrum of O1s showing the presence of several oxygenated functional groups on the MWCNT after acid treatment.

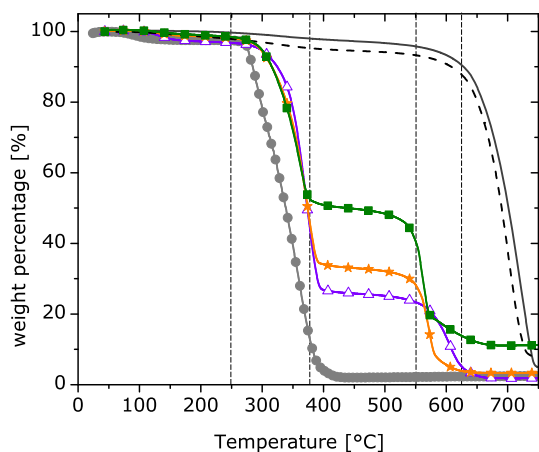


Fig. 6. TGA curves of the MWCNT-OH (—), MWCNT-Br (—), PMMA-grafted-MWCNT #2 (■), #3 (★), #4 (△) and pure PMMA (●).

during the grafting process. A possible solution would have been to disperse the modified nanotubes in toluene ( $\theta$  solvent of PMMA) in order to disfavor the entanglement of the polymer chains. However, the MWCNT could not be dispersed in this solvent. Fig. 6 plots the TGA curves of the unmodified MWCNT and PMMA-grafted-MWCNT samples obtained from route 2. The TGA curves show five main changes as a function of the temperature. Below 250 °C only the decomposition of adsorbed moisture or loosely attached functional groups may take place. Between 250 °C and 385 °C the rapid weight decrease may readily be attributed to the decomposition of PMMA polymer on the tube wall as well as oxygenated functional groups playing the role of anchorage interface. Between 385 °C and 550 °C it is noticeable that no weight loss is observed for MWCNT-OH and MWCNT-Br whereas at 550 °C a significant weight reduction occurs on the nanocomposite functionalized with PMMA. It is worthy to note that the combustion of the MWCNT-OH and MWCNT-Br takes place at much higher temperature, i.e. 620 °C. Such difference of the combustion temperature could be attributed to the higher reactivity of the functionalized MWCNT which initiate the combustion process far beyond that observed on the pristine MWCNT.

In addition, the weight fraction loss of PMMA in sample #3 was amounted to 65.5%, while it was 71.5% in #4 sample. These results indicate that the functionalization of MWCNT can be well-controlled by the feed ratio of MMA (Table 1). Indeed, the amount of monomer was doubled in sample #4, thus leading to

longer polymer chains and subsequently a higher PMMA weight loss observed by TGA. Furthermore, increasing the volume of solvent used for the polymerization reaction has also an effect on the density of the grafted polymer. Indeed, increasing the volume of solvent five times for sample #2 (vs. sample #3) lead to the reduction of the weight fraction of polymer from 65.5% (3) to 49.1% (2). This result is explained by the fact that decreasing the concentration of monomer during the polymerization process causes a decrease of the polymerization kinetic, thus leading to smaller polymer chains and therefore the thickness of the polymer layer on MWCNT surface is also reduced.

In order to confirm the PMMA grafting, FTIR analyses were also carried out (Fig. 7). For clarity, only the range from 1200 to 1800  $\text{cm}^{-1}$  is shown. The overall FTIR spectrum from 400 to 4000  $\text{cm}^{-1}$  is given in SI. As shown in Fig. 7, the absorption signal of carbonyl band at around 1730  $\text{cm}^{-1}$  is barely detected for the samples MWCNT-Br and MWCNT-OH while it is strongly visible for MWCNT-PMMA. Moreover, one can notice that the density of the peak at 1730  $\text{cm}^{-1}$  increases with increasing the density of the polymer (Table 1). Finally, the C=C absorption band observed around 1630  $\text{cm}^{-1}$  for MWCNT-PMMA samples confirmed the success of the functionalization.

### 3.2. Mechanical and surface properties of composite coating

#### 3.2.1. Bulk mechanical properties of the composite coatings

Fig. 8 displays Young's modulus and hardness versus

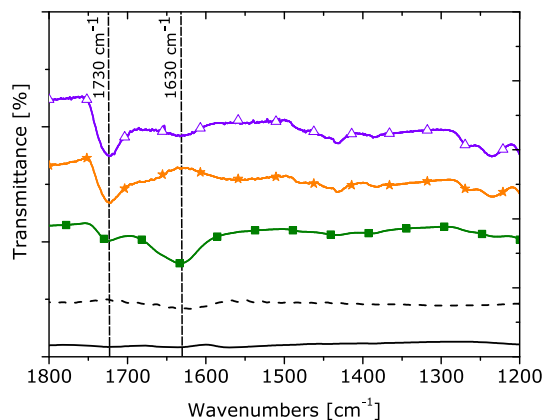
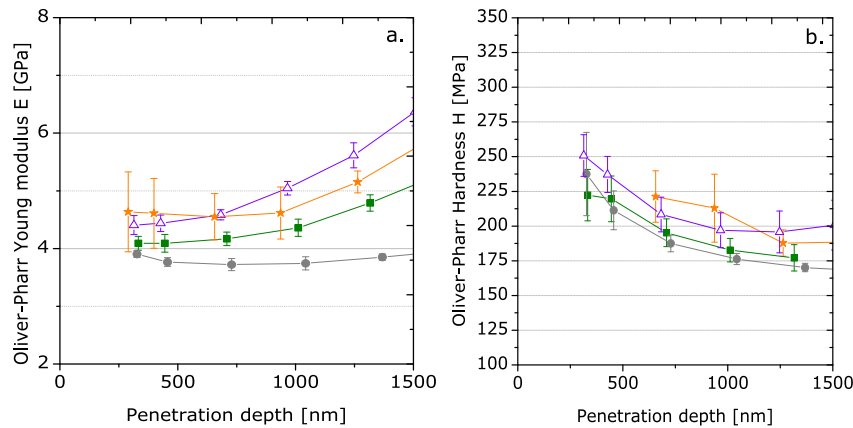


Fig. 7. FTIR spectra recorded for the MWCNT-OH (—), MWCNT-Br (—), PMMA-grafted-MWCNT #2 (■), #3 (★), #4 (△).



**Fig. 8.** Mechanical properties of (●) pure PMMA coating and PMMA nanocomposite coatings with 2wt.% PMMA-grafted-MWCNT (■) #2 /PMMA, (★) #3/PMMA and (△) #4/PMMA obtained by nanoindentation: (a) Young's modulus and (b) Hardness versus depth.

penetration depth of a Berkovich tip from nanoindentation experiments for PMMA-grafted-MWCNT/PMMA and a PMMA reference coating. The data were fitted with the Oliver-Pharr model with a Poisson's ratio value of 0.35 [30]. As this model is dedicated to elastic–plastic materials gradual increasing loading cycles were performed (as described in the Materials section) to avoid the viscoelastic effect during the analysis. The coating thicknesses range between 10 and 15  $\mu\text{m}$  that is why only the first micron will be considered to get only the intrinsic properties of the coating. Moreover, results in the first 500 nm depth are not considered as it is mostly due to the tip's apex defect and the surface roughness effect. The Young's modulus  $E$  of the PMMA-grafted-MWCNT/PMMA coatings are quite alike (due to the error bar) and slightly higher than pure PMMA (~20%). From these curves we can estimate the value for which strain starts in the bulk of the composite from the calculation of the ratio  $H/E$ ,  $H$  being the calculated hardness and  $E$  the calculated Young modulus. For each studied coatings the value is estimated at a penetration depth of 750 nm:  $H/E$  is rather similar ( $H/E \approx 0.047$ ) which entails that the yielding strains are alike for these composites.

### 3.2.2. Surface properties

Tribological and mechanical tests were performed for the samples coated with PMMA reinforced with 2wt% of PMMA-

grafted-MWCNT with various weights' fraction of grafted PMMA on the MWCNT surface. According to the TGA measurements the weight fraction loss of grafted PMMA was 49%, 66% and 71% for samples #2, #3 and #4 respectively (Table 2 and Fig. 6). The solution for coating was prepared by solution mixing method. Control sample coated with pure PMMA was prepared by the same method. Tribological measurements were performed to characterize the influence of PMMA-grafted-MWCNT fillers on coating response to shearing. Fig. 9 plots the evolution of the rear contact angle  $\omega$  versus the ratio  $a/R$  proportional to imposed surface strain. The yielding plateau of the PMMA coating starts around 0.35/0.4 which is a classical value. The yielding plateau of the reinforced coatings starts at a higher value (~0.5). The elastic–plastic range has increased for this latter. Pictures of the contacts for  $a/R = 0.35$ , where  $a$  is the contact radius and  $R$  the radius of the indenter, clearly show this difference. The more the TGA weight loss is high, the more the scratch contact shape turns to an elastic sliding contact. The weight loss may be related to the mean PMMA chain length grafted to MWCNT: the highest it is, the less plastic the coating behavior is at a given contact strain.

From these experimental results we can calculate the apparent friction coefficient  $\mu_{\text{app}}$  which is the ratio of the measured friction force  $F_t$  and the imposed normal load  $F_n$ . Fig. 10a displays the results for each coating. It is important to notice that for a mean

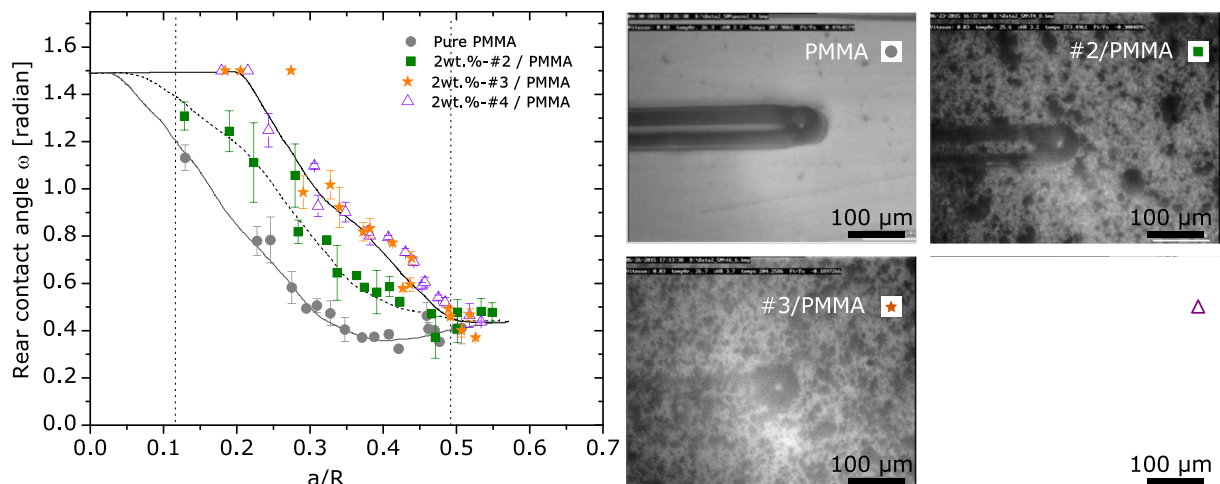


**Fig. 9.** Evolution of the rear contact angle versus the ratio  $a/R$  ( $R = 98 \mu\text{m}$ ) for coatings of pure PMMA (●) and PMMA nanocomposites with 2wt.% PMMA-grafted-MWCNT (■) #2/PMMA, (★) #3/PMMA and (△) #4/PMMA; selected images at  $a/R = 0.35$ .



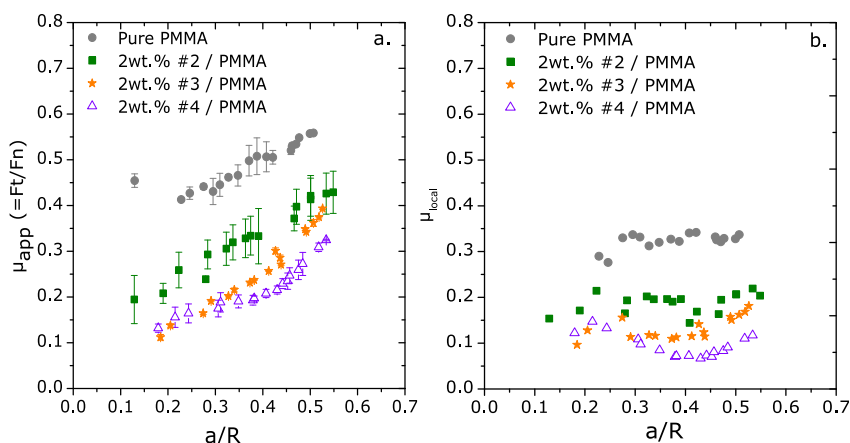


**Fig. 10.** Evolution of the apparent friction coefficient  $\mu_{\text{app}}$  (a) and the local friction coefficient  $\mu$  (b) versus the ratio  $a/R$  ( $R = 98 \mu\text{m}$ ) for coatings of pure PMMA (●) and PMMA nanocomposites with 2wt.% PMMA-grafted-MWCNT (■) #2/PMMA, (★) #3/PMMA and (△) #4.

coating thickness of  $15 \mu\text{m}$  and a indenter radius of  $98 \mu\text{m}$  the critical  $(a/R)_c$  ratio over which the substrate effect is no more negligible is approximately 0.2 (estimated from Pythagorean theorem). We can easily observed that the reinforcement of PMMA coating with PMMA-grafted-MWCNT filler reduce the apparent friction coefficient by at least half. The apparent friction coefficient is the result of the sum of two phenomena: the friction due to the matter amount pushed in front of the tip and the friction linked to the shearing of the interfacial layer between the indenter and the surface. We call the latter local friction coefficient,  $\mu_{\text{loc}}$ , and it can be deduced from the experimental results by a surface flow line model developed by previous work [31]. Fig. 10b plots the local friction coefficient  $\mu_{\text{loc}}$  versus the ratio  $a/R$ . It clearly appears that the local friction is affected by the presence of PMMA-grafted-PMMA fillers and is highly reduced: the MWCNT structure acts as lubricant during shearing. It is important to note that the grafted-PMMA chains act as entanglements and probably gives a strain-hardening effect into the stress-strain behavior, giving a benefit for the decreasing of the ductile plowing part [32]. The sliding between the outer graphite concentric layer coated with PMMA and the rest of the graphitic layer could be advanced to explain such phenomenon.

#### 4. Conclusion

In summary, acid treated MWCNT surface has been successfully modified with PMMA chains via ATRP using a “grafting from” approach. The presence of oxygenated functional groups on the MWCNT surface plays the role of anchorage interface for the subsequence PMMA layer with high adhesion strength. In addition, this strategy can be employed to grow a large range of polymers from the MWCNT surface by changing the monomer type, the feed ratio or the volume of solvent used as a reaction medium. The resulting nanocomposites were readily dispersed in organic solvents and can be used as reinforcement fillers in the preparation of PMMA composite films. A good distribution of the fillers in the PMMA matrix was achieved thanks to the surface grafting with PMMA chains.

Addition of MWCNT-grafted-PMMA to PMMA coating layer can decrease the apparent friction coefficient depending on the thickness of the PMMA layer on MWCNT walls. On the other hand, the coefficient of friction decreases relatively with the increase in the weight fraction of polymer grafted on the surface of MWCNT.

#### Acknowledgments

The authors would like to acknowledge the “Polymer characterization”, “Electron microscopy” and “Micro Nano mechanics” platforms of the ICS as well as the “Thermal” platform of the ICPEES for TGA measurements.

#### Appendix A. Supplementary data

Supplementary data related to this article can be found at <http://dx.doi.org/10.1016/j.matchemphys.2016.03.021>.

#### References

- [1] B.J. Briscoe, S.K. Sinha, Tribology of polymeric solids and their composites, in: G. Stachowiak (Ed.), *Wear - Materials, Mechanisms and Practice*, John Wiley & sons, Chichester, England, 2005, pp. 223–267.
- [2] S. Anandhan, S. Bandyopadhyay, Polymer nanocomposites: from synthesis to applications, in: J. Cuppoletti (Ed.), *Nanocomposites and Polymers with Analytical Methods*, Intech, 2011, p. 3.
- [3] K. Friedrich, A.K. Schlarb, in: B.J. Briscoe (Ed.), *Tribology of Polymeric Nanocomposites*, Tribology and Interface Engineering Series, 55, Elsevier Science, Series, United Kingdom, 2008.
- [4] I. Demirci, C. Gauthier, R. Schirrer, Mechanical analysis of the damage of a thin polymeric coating during scratching: role of the ratio of the coating thickness to the roughness of a scratching tip, *Thin Solid Films* 479 (2005) 207–215.
- [5] S. Iijima, Helical microtubules of graphitic carbon, *Nature* 354 (1991) 56–58.
- [6] Z. Jia, Z. Wang, C. Xu, J. Liang, B. Wei, D. Wu, S. Zhu, Study on poly(methyl methacrylate)/carbon nanotube composites, *Mat. Sci. Eng. A* 271 (1999) 395–400.
- [7] P.C. Ma, N.A. Siddiqui, G. Marom, J.K. Kim, Dispersion and functionalization of carbon nanotubes for polymer-based nanocomposites: a review, *Compos Part A* 41 (2010) 1345–1367.
- [8] X.L. Xie, Y.W. Mai, X.P. Zhou, Dispersion and alignment of carbon nanotubes in polymer matrix: a review, *Mat. Sci. Eng. R. Rep.* 49 (2005) 89–112.
- [9] L. Vaisman, H.D. Wagner, G. Marom, The role of surfactants in dispersion of carbon nanotubes, *Adv. Coll. Inter Sci.* 128 (2006) 37–46.
- [10] J. Zou, L. Liu, H. Chen, S.I. Khondaker, R.D. McCullough, Q. Huo, L. Zhai, Dispersion of pristine carbon nanotubes using conjugated block copolymers, *Adv. Mat.* 20 (2008) 2055–2060.
- [11] V.M. Lahelin, A. Vesterinen, A. Nykänen, J. Ruokolainen, J. Seppälä, In situ polymerization of methyl methacrylate/multi-walled carbon nanotube composites using cationic stearyl methacrylate copolymers as dispersants, *Eur. Polym. J.* 47 (2011) 873–881.
- [12] M.L. Polo-Luque, B.M. Simonet, M. Valcárcel, Functionalization and dispersion of carbon nanotubes in ionic liquids, *Trends Anal. Chem.* 47 (2013) 99–110.
- [13] L. Zhao, Y. Li, X. Cao, J. You, W. Dong, Multifunctional role of an ionic liquid in melt-blended poly(methyl methacrylate)/multi-walled carbon nanotube nanocomposites, *Nanotechnology* 23 (2012) 255702 (8pp).
- [14] V.T. Le, C.L. Ngo, Q.T. Le, T.T. Ngo, D.N. Nguyen, M.T. Vu, Surface modification and functionalization of carbon nanotube with some organic compounds, *Adv. Nat. Sci. Nanosci. Nanotechnol.* 4 (2013) 035017.
- [15] X. Pan, X. Bao, The effects of confinement inside carbon nanotubes on catalysis, *Acc. Chem. Res.* 44 (2011) 553–562.



- [16] C. Pham-Huu, M.J. Ledoux, Carbon nanomaterials with controlled macroscopic shapes as new catalytic materials, *Top. Catal.* 40 (2006) 49–63.
- [17] J.P. Tessonnier, D.S. Su, Recent progress on the growth mechanism of carbon nanotubes: a review, *ChemSusChem* 4 (2011) 824–847.
- [18] P. Serp, M. Corrias, P. Kalck, Carbon nanotubes and nanofibers in catalysis, *Appl. Catal. A* 253 (2003) 337–358.
- [19] D.S. Su, S. Perathoner, G. Centi, Nanocarbons for the development of advanced catalysts, *Chem. Rev.* 113 (2013) 5782–5816.
- [20] M. Salami-Kalajahi, V. Haddadi-Asl, F. Behboodi-Sadabad, S. Rahimi-Razin, H. Roghani-Mamaqani, Properties of PMMA-carbon nanotubes nanocomposites prepared by “grafting through” method, *Polym. Compos.* 33 (2012) 215–224.
- [21] H. Kong, C. Gao, D. Yan, Controlled functionalization of multiwalled carbon nanotubes by in situ atom transfer radical polymerization, *J. Am. Chem. Soc.* 126 (2004) 412–413.
- [22] G.L. Hwang, Y.-T. Shieh, K.C. Hwang, Efficient load transfer to polymer-grafted multiwalled carbon nanotubes in polymer composites, *Adv. Funct. Mat.* 14 (2004) 487–491.
- [23] M. Wang, K.P. Pramoda, S.H. Goh, Enhancement of the mechanical properties of poly(styrene-co-acrylonitrile) with poly(methyl methacrylate)-grafted multiwalled carbon nanotubes, *Polymer* 46 (2005) 11510–11516.
- [24] D. Blond, V. Barron, M. Ruether, K.P. Ryan, V. Nicolosi, W.J. Blau, J.N. Coleman, Enhancement of modulus, strength, and toughness in poly(methyl methacrylate)-based composites by the incorporation of poly(methyl methacrylate)-functionalized nanotubes, *Adv. Funct. Mat.* 16 (2006) 1608–1614.
- [25] B. Dong, Z. Yang, Y. Huang, H.-L. Li, L. Liu, F.-Y. Yan, Preparation and tribological properties of poly(methyl methacrylate)/multi-walled carbon nanotubes composites, *J. Mat. Sci.* 40 (2005) 4379–4382.
- [26] J. Kim, H. Im, M.H. Cho, Tribological performance of fluorinated polyimide-based nano-composite coatings reinforced with PMMA-grafted-MWCNT, *Wear* 271 (2011) 1029–1038.
- [27] F. Mammeri, J. Teyssandier, C. Darche-Dugaret, S. Debacker, E. Le Bourhis, M.M. Chehimi, Carbon nanotube–poly(methyl methacrylate) hybrid films: preparation using diazonium salt chemistry and mechanical properties, *J. Colloid Interface Sci.* 433 (2014) 115–122.
- [28] C. Gauthier, A.-L. Durier, C. Fond, R. Schirrer, Scratching of a coated polymer and mechanical analysis of a scratch resistance solution, *Tribol. Int.* 39 (2006) 88–98.
- [29] C. Gauthier, S. Lafaye, R. Schirrer, Elastic recovery of a scratch in a polymeric surface: experiments and analysis, *Tribol. Int.* 34 (2001) 469–479.
- [30] W.C. Oliver, G.M. Pharr, Measurement of hardness and elastic modulus by instrumented indentation: advances in understanding and refinements to methodology, *J. Mat. Res.* 19 (2004) 3–20.
- [31] S. Lafaye, C. Gauthier, R. Schirrer, A surface flow line model of a scratching tip: apparent and true local friction coefficients, *Tribol. Int.* 38 (2005) 113–127.
- [32] J.L. Bucaille, C. Gauthier, E. Felder, R. Schirrer, The influence of strain hardening of polymers on the piling-up phenomenon in scratch tests: experiments and numerical modelling, *Wear* 260 (2006) 803–814.